Kinetics of deposition of oriented superdisks

Branislav N. Aleksić,[1,2] N. M. Švrakić,[2] and M. Belić[1]
[1]*Texas A&M University at Qatar, Doha, Qatar*
[2]*Institute of Physics Belgrade, University of Belgrade, Belgrade, Serbia*
(Received 27 May 2013; published 6 December 2013)

We use numerical Monte Carlo simulation to study the kinetics of the deposition of oriented superdisks, bounded by the Lame curves of the form $|x|^{2p} + |y|^{2p} = 1$ on a regular planar substrate. Recently, it was shown that the maximum packing density as well as jamming density ρ_J exhibit a discontinuous derivative at $p = 0.5$ when the shape changes from convex to concave form. By careful examination of the late-stage approach to the jamming limit, we find that the leading term in the temporal development is also nonanalytic at $p = 0.5$ and offer heuristic excluded-area arguments for this behavior.

DOI: 10.1103/PhysRevE.88.062112 PACS number(s): 02.50.−r, 68.43.Mn, 05.10.Ln, 05.70.Ln

Deposition, or adsorption, of extended objects at different surfaces is of considerable interest for a wide range of applications in biology, nanotechnology, device physics, physical chemistry, and materials science [1,2]. Typically, such objects range in size from submicrometer scale down to nanometer scale, and, depending on the application in question, the objects could be polymers, globular proteins, nanotubes, DNA segments, or general geometrical shapes, such as disks, polygons, etc. Early studies have focused on the deposition of simple regular shapes (lines and needles) on spatially homogeneous regular substrates [3], and the main issue was the effect of shape, size, orientation, and symmetry of the depositing objects on the late-stage kinetics of this process.

A typical physical situation is that the particles (objects) are randomly deposited on the target surface with uniform flux and that there are no equilibrium processes active at the surface. Because of this, the final density of the deposited objects, after which no additional deposition is possible, is less than the maximum packing density. This final, or jamming density ρ_J, has recently been studied [4] for objects of different geometrical shapes and symmetries, and it was shown that ρ_J exhibits singularity when the shape changes from convex to concave. In a separate study of the densest packing of nonoverlapping objects [5], the maximal packing density is found to be nonanalytic at the point when objects become noncircular. Additionally, it was found that the change in shape away from rotational symmetry influences packing characteristics in a nontrivial way.

Theoretically, several models have been developed to capture the basic physics of deposition, and by far, the most studied is that of random sequential adsorption (RSA) [3]. In this model, particles (objects) are sequentially deposited on the randomly chosen site on the substrate. When deposited, such objects are irreversibly and permanently attached to that site. If the randomly chosen site for deposition is already occupied or the objects overlap due to their size or shape, the deposition is rejected, the particle is discarded, and the deposition is next attempted at a different randomly chosen site. Note that, in this process, object-object and object-substrate interactions are modeled solely by geometrical and other features included in the deposition procedure [6–16].

Two main properties are of particular experimental and theoretical interest in this process: (i) the final jamming density of objects and (ii) the leading temporal approach to the jammed state. This second property prominently features in an experimental situation where it is important to understand the process of approaching various specific morphological properties as the deposit is formed, for example, avoiding contact. Examples include depositions on prepatterned surfaces [17–19], nanoparticle sintering [20], or in inkjet printing technology [21] where the evolution of surface morphology plays a major role. Although the properties of the final jammed state as a function of geometry and size of the depositing objects are reasonably well understood [4], the kinetic properties of the approach to this state have not been studied extensively (see, for instance, concluding remarks in Ref. [13]). It is the purpose of the present paper to address this question.

In this paper, we consider the kinetics of the deposition of oriented "superdisks" on homogeneous planar substrates. Such shapes in two dimensions are defined by the expression $|x|^{2p} + |y|^{2p} \leqslant 1$, where p is deformation parameter with values $p \in (0,\infty)$. As p varies, the shape changes from "cross" ($p = 0$), to square ($p = 0.5$), to circle ($p = 1$), to "diamond" ($p = \infty$) as illustrated in Fig. 1.

Note that, for $p < 0.5$, the depositing object is concave, of general asteroid shape, and then becomes convex for $p > 0.5$. Clearly, $p = 0.5$ is the special point in this respect (see below). Also, when $p = 1$, the shape is a circle. For all $p > 1$, we get the family of objects with quadratic symmetry, whereas, for $p < 1$, the resulting family of objects also has quadratic symmetry but is rotated by $\pi/4$ with respect to the first group [5]. It is clear, generally, that by changing the deformation parameter p, one can control both the convexity and the symmetry of the object.

The deposition proceeds via the standard RSA algorithm: The point on the surface is randomly chosen to place the center of the object. If the object can "fit" at this point without overlapping with neighboring deposited objects, it is placed there. Otherwise, it is discarded, and the next deposition is attempted at a different randomly chosen point. In our simulation, we only used oriented objects.

At the very early stages of the deposition, we expect that the density of the deposited objects will grow linearly with time since almost any randomly chosen point for the deposition attempt will be unoccupied. However, as more and more

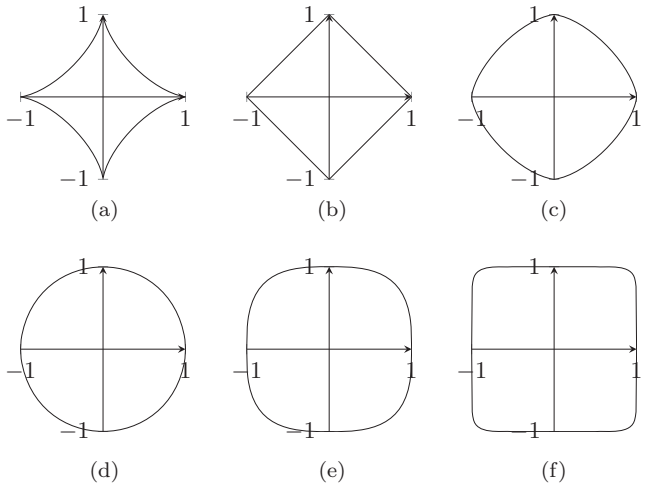

FIG. 1. Superdisk shapes for different values of deformation parameter p. (a) $p = 0.35$, (b) $p = 0.5$, (c) $p = 0.75$, (d) $p = 1.0$, (e) $p = 1.5$, and (f) $p = 5.0$. Note the change in shape from concave to convex at $p = 0.5$.

objects are deposited, it becomes harder to find an available spot to place an object without overlap, and the density of deposited objects $\rho(t)$ grows much more slowly, until it reaches jamming density ρ_J after which no more objects can be placed on the substrate. This final jammed-state configuration is not unique, and objects do not cover the substrate with maximum packing density [3]. Indeed, the jamming density, or the density of deposited particles per unit area, is simply related to the jamming coverage or the fraction of the covered area by the simple relation $A(p)\rho_J(p)$, where $A(p)$ is the area of the superdisk (see below) and we have explicitly indicated p dependence of the relevant quantities. Of course, the details of the approach to the jammed state, i.e., the late-stage deposition kinetics as well as the jamming density itself, will depend on the shape of the objects. Recall that this shape can be continually tuned by varying the deformation parameter p. As mentioned, in a recent study, Gromenko and Privman [4] have shown that the jamming density ρ_J is nonanalytic at $p = 0.5$, i.e., when the object's shape changes from convex to concave.

Turning back to the approach to the jamming density, recall that, in RSA, the process is described by the standard Pomeau [22] and Swendsen [23] conjectures, which give asymptotic results for oriented simple shapes that are in agreement with numerical simulations [24]. These conjectures, however, may not be correct for nonoriented objects [25,26]. In the rest of this paper, we describe the numerical procedure used and the results obtained for the deposition kinetics of oriented superdisks with the deformation parameter in the range of $0 \leqslant p \leqslant 1$.

In our Monte Carlo (MC) procedure, the substrate was of the size $500D \times 500D$, where D is the typical "diameter" of the depositing object [5]. In our simulation, $D = 2$. Once the point for the center of the object is selected randomly on this substrate, we tested if the whole object can fit without overlap with neighboring objects already deposited. It is not necessary to check overlapping with all neighbors but only with nearby points with centers not closer than D from the new point. Overlap testing is a computationally "expensive" operation,

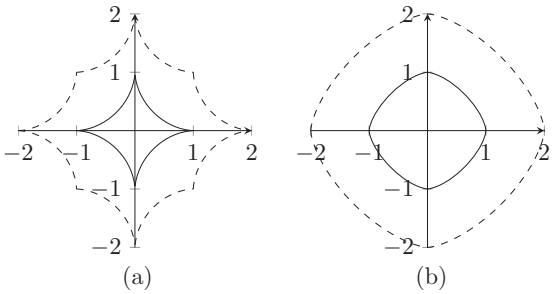

FIG. 2. Exclusion regions for concave and convex superdisks (outer envelopes). The example illustrates cases with (a) $p = 0.3$ and (b) $p = 0.75$.

so this approach makes simulation much faster than checking all previously deposited points for every new candidate point. We performed two implementations, one in the "C" and one in the "JAVA" programming languages. It appears that JAVA is more reliable as a random number generator.

With very simple objects, such as line segments and the like, this test is straightforward but becomes more involved in the case of superdisks. Namely, each superdisk of the form $|x|^{2p} + |y|^{2p} \leqslant 1$ has the area,

$$A(p) = 4\frac{\Gamma^2\left(1+\frac{1}{2p}\right)}{\Gamma\left(1+\frac{1}{p}\right)}, \tag{1}$$

where Γ is the standard Γ function. No point encompassed by this area can be shared with any other superdisk (nonoverlap condition). This means that there is an exclusion region around the deposited superdisk within which no center of another superdisk can be placed. For example, when $p = 1$, the object is a circle with a unit radius with an area of $A(1) = \pi$, and the corresponding exclusion region is a circle but with a radius equal to 2 and an area of 4π.

In general, the exclusion region for the convex superdisks of the form $|x|^{2p} + |y|^{2p} \leqslant 1$ is another superdisk of the form $|x|^{2p} + |y|^{2p} \leqslant 2^{2p}$, and the area of this region is $A_{cx} = 4A(p)$, where $A(p)$ is given by (1) and the subscript "cx" indicates that $p \geqslant 0.5$, i.e., the object is convex. Within this region, no center of another superdisk can be placed.

For concave superdisks, the situation is slightly more involved. The exclusion region is shown in Fig. 2. Its boundary consists of the external envelope formed by four superdisks centered at the corners of the original superdisk $|x|^{2p} + |y|^{2p} \leqslant 1$.

The exclusion area of this region is calculated easily and is given by $A_{cc} = 4 + 2A(p)$, where $A(p)$ is given by Eq. (1) and the subscript "cc" indicates that $p \leqslant 0.5$, i.e., the superdisk is concave. Recall that $A(0.5) = 2$ so that $A_{cx}(p = 0.5) = A_{cc}(p = 0.5)$, and the exclusion areas are equal as expected. However, the derivative of the excluded area has a discontinuity at $p = 0.5$. This clearly is visible in Fig. 3. Solid lines mark the parts of A_{cc} and A_{cx} that must be used to determine the real exclusion region. The dashed lines are their nonphysical continuations.

This nonanalyticity of the excluded area is the origin of the observed singularity in both the jammed state [4] and the maximum packing state [5] of the superdisks at $p = 0.5$.

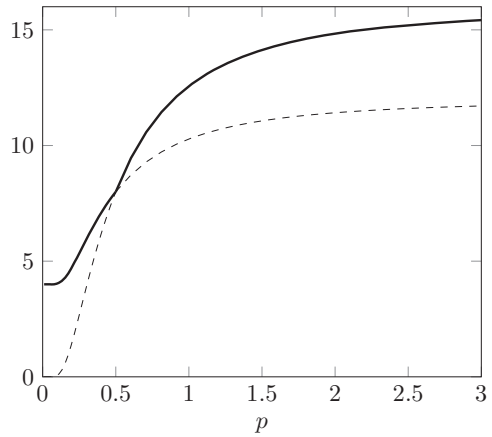

FIG. 3. The area (size) of the exclusion regions is marked by the solid line.

To investigate the kinetics of RSA deposition of superdisks, we performed 100 MC runs for each value of $0 \leqslant p \leqslant 1$ with each run typically of several 10^9 steps, until the jamming limit was reached. We plausibly expect [12,27] that the approach of the coverage density to its value at the jammed state is of the exponential form

$$\rho(t,p) = \rho_J(p) - Q(p)e^{-t\sigma(p)}, \tag{2}$$

where Q and σ are parameters to be determined and their (possible) p dependence is explicitly indicated. The normalized jamming limit shows nonanalytic behavior at $p = 0.5$ as explained above [4]. The plot of the normalized jamming limit faithfully reproduces the result previously obtained by Gromenko and Privman illustrated in Fig. 3 of Ref. [4].

This can also be seen on the plot of the coverage density, shown below in Fig. 4.

Turning to the time dependence, we plot $\ln[\rho_J - \rho(t)]$ vs time for several values of parameter p as shown in Fig. 5.

Inspection of this graph shows: (i) that the parameter σ from Eq. (2) has no dependence on p, and we get $\sigma = 3.5 \times 10^{-3}$, and (ii) that $Q(p)$, the prefactor in front of the exponential approach in Eq. (2), depends on the deformation parameter p in a nontrivial way.

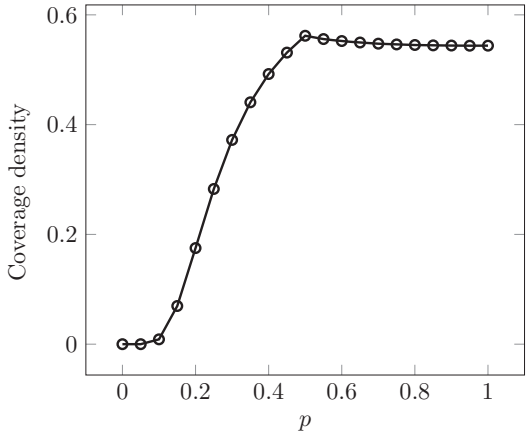

FIG. 4. Coverage density as a function of deformation parameter p.

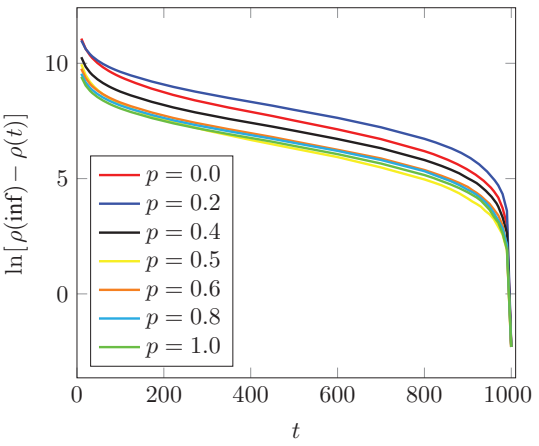

FIG. 5. (Color online) Approach to the jamming density with time for several values of the deformation parameter p. The linear part can be approximated by the line of the form $-\sigma t + \ln[Q(p)]$.

This is not entirely unexpected as is known [27] that with the RSA deposition of line segments on the substrate, the corresponding prefactor is inversely proportional to the length of the segment. In this simple situation, the exclusion area is simply the length of the segment. In our case, the connection is more complicated. The plot of $Q(p)$ vs p is shown in Fig. 6.

This term is clearly nonanalytic at $p = 0.5$ (square object). We believe that this reflects nonanalyticity of the exclusion area for this value of p, which is, itself, a consequence of the change in convexity of the deposited objects.

In conclusion, we have studied the time dependence of the deposition of oriented superdisks of various shapes on homogeneous substrates. Our results indicate that, in addition to maximum packing density and jamming density, the leading term in late-stage deposition also shows nonanalytic behavior when depositing objects change their shapes from convex to concave. Intuitively, one would expect that the convexity of the depositing object would become more important in late-stage deposition kinetics as they pack closer and closer, and the details of their shapes and the size of the exclusion area begin to play more prominent roles. The study of this effect for nonoriented superdisks is currently under way.

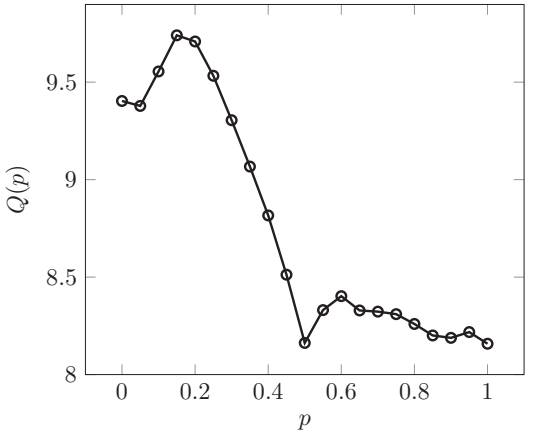

FIG. 6. Plot of the prefactor of the exponential approach to the jamming limit Eq. (2) shows nontrivial dependence on p and a singularity at $p = 0.5$.

This paper was made possible by NPRP Grants No. 09-462-1-074 and No. 5-674-1-114 from the Qatar National Research Fund (a member of the Qatar Foundation). Work at the Institute of Physics Belgrade was supported by the Ministry of Science of the Republic of Serbia under Projects No. OI 171006 and No. ON 171017.

[1] *Nonequilibrium Statistical Mechanics in One Dimension*, edited by V. Privman (Cambridge University Press, Cambridge, UK, 1997) (a collection of review articles).
[2] V. Privman, Colloids Surf. A **165**, 1 (2000) (a collection of review articles).
[3] J. W. Evans, Rev. Mod. Phys. **65**, 1281 (1993).
[4] O. Gromenko and V. Privman, Phys. Rev. E **79**, 042103 (2009).
[5] Y. Jiao, F. H. Stillinger, and S. Torquato, Phys. Rev. Lett. **100**, 245504 (2008).
[6] V. Privman, J. Adhes. **74**, 421 (2000).
[7] J.-S. Wang, P. Nielaba, and V. Privman, Physica A **199**, 527 (1993).
[8] N. A. M. Araujo, A. Cadilhe, and V. Privman, Phys. Rev. E **77**, 031603 (2008).
[9] N. A. M. Araujo and A. Cadilhe, Phys. Rev. E **73**, 051602 (2006).
[10] P. Nielaba and V. Privman, Mod. Phys. Lett. B **6**, 533 (1992).
[11] J.-S. Wang, P. Nielaba, and V. Privman, Mod. Phys. Lett. B **7**, 189 (1993).
[12] M. C. Bartelt and V. Privman, Phys. Rev. A **44**, R2227 (1991).
[13] A. Cadilhe, N. A. M. Araujo, and V. Privman, J. Phys.: Condens. Matter **19**, 065124 (2007).
[14] O. Gromenko, V. Privman, and M. L. Glasser, J. Comput. Theor. Nanosci. **5**, 2119 (2008).
[15] O. Gromenko and V. Privman, Phys. Rev. E **79**, 011104 (2009).
[16] J. J. Gonzalez, P. C. Hemmer, and J. S. Hoye, Chem. Phys. **3**, 228 (1974).
[17] S. Minko, M. Muller, M. Motornov, M. Nitschke, K. Grundke, and M. Stamm, J. Am. Chem. Soc. **125**, 3896 (2003).
[18] L. Ionov, S. Minko, M. Stamm, J. F. Gohy, R. Jerome, and A. Scholl, J. Am. Chem. Soc. **125**, 8302 (2003).
[19] A. Kiriy, G. Gorodyska, S. Minko, C. Tsitsilianis, W. Jaeger, and M. Stamm, J. Am. Chem. Soc. **125**, 11202 (2003).
[20] M. Layani and S. Magdassi, J. Mater. Chem. **21**, 15378 (2011).
[21] K. Balantrapu, M. McMurran, and D. Goia, J. Mater. Res. **25**, 821 (2010).
[22] Y. Pomeau, J. Phys. A **13**, L193 (1980).
[23] R. H. Swendsen, Phys. Rev. A **24**, 504 (1981).
[24] B. J. Brosilow, R. M. Ziff, and R. D. Vigil, Phys. Rev. A **43**, 631 (1991).
[25] V. Privman, J.-S. Wang, and P. Nielaba, Phys. Rev. B **43**, 3366 (1991).
[26] G. Tarjus and P. Viot, Phys. Rev. Lett. **67**, 1875 (1991).
[27] S. S. Manna and N. M. Švrakić, J. Phys. A **24**, L671 (1991).